Journal of Theoretical and Applied Mechanics, Sofia, Vol.53 (2023) pp. 49-65
INTERDISCIPLINARY TOPICS

MODELING OF CUTTING FORCE AND POWER CONSUMPTION USING ANN AND RSM METHODS IN TURNING OF AISI D3: COMPARATIVE STUDY AND PRECISION BENEFIT

KHAOULA SAFI[1*], MOHAMED ATHMANE YALLESE[1], SALIM BELHADI[1], TAREK MABROUKI[2], SALIM CHIHAOUI[1]

[1]*Université 8 Mai 1945, Guelma, Laboratoire (LMS), Algérie*
[2]*Université de Tunis El Manar, ENIT, Laboratoire (MAI), Tunisie*

[Received: 14 October 2021. Accepted: 17 October 2022]

doi: https://doi.org/10.55787/jtams.23.53.1.49

ABSTRACT: The present work deals with the optimization of cutting parameters when turning D3 steel using a CVD multi-layer coated carbide tool (Al_2O_3+TiC+TiCN). For that, response surface methodology (RSM) and artificial neural network (ANN) were adopted for the modeling of cutting force (F_z) and cutting power evolutions (P_c). The applied precited approaches were also compared and their results were discussed. Moreover, a design of experimental (DoF) based on Taguchi L16 ($4 \wedge 3\ 2 \wedge 1$) method was adopted. This has helped to illustrate the relationship between cutting parameters (tool radius, cutting speed, feed rate and cutting depth) and selected responses which are cutting force and cutting power. The results revealed that the ANN and RSM exhibited very good accuracy with experimental data. However, the ANN prediction model provides the maximum benefit in terms of precision compared to the RSM model. For (F_z and P_c) the benefit is (7.5 and 16.3)%, respectively.

KEY WORDS: AISI D3, turning, cutting force, coated carbide (CVD), RSM, ANN.

NOMENCLATURE

r:	Tool nose radius (mm)	P_c:	Power consumed [W]
V_c:	Cutting speed [m/min]	RSM:	Response surface methodology
f:	Feed rate [mm/rev]	ANN:	Artificial neural network
ap:	Depth of cut [mm]	ANOVA:	Analysis of variance
F_z:	Cutting force [N]		

1 INTRODUCTION

Nowadays, the main goal of the manufacturing industry is to reduce material processing costs by minimizing consumption of power and also respecting workpiece

*Corresponding author e-mail: safikhaoula40@gmail.com

qualification criteria. Among material process, it can be mentioned that material removal by cutting tools plays always an important role in manufacturing. Enhancing the machinability of some materials is staying among years essential in machining processes [1, 2]. For example, the high alloy steels which are widely used in various industrial fields thanks to their resistance to wear, their machinability is not yet well controlled to reach the respect of some qualification criteria in production. These materials are widely needed for the production of dies, cutting and stamping equipment, punches, drawing dies, profiling rollers, wood working tools and thread rolling [3]. In order to optimize the cutting parameters, the RSM method is commonly used. Its main advantage is that it can easily quantify both the main parameters and the interactions that influence the process output parameters. Also, it is very effective in determining prediction models that will be used to optimize the responses and determine the optimal operating conditions according to the desired objectives [4]. Nevertheless, it presents some difficulty when dealing with non-linear phenomena. This is the reason why other techniques based on artificial intelligence (AI) have been investigated. The ANN approach is one of the techniques of computer modeling capable of modeling a non-linear problem in an efficient way thanks to its simplicity, its precision and its rapidity of treatment [5].

In this context, several studies that aim to compare the performance of modeling methods in terms of precision were carried out [6–8]. Gaitonde et al. [9] used the method RSM to develop an empirical model for the prediction of some machining performance parameters (F_z, P_c, Kc, Ra and VB). The study was realized on an AISI D2 steel using ceramic and Wiper tools. Süleyman Neşeli et al. [10] have made an experimental study on the influence of cutting parameters and tool geometry on Ra evolution during turning of AISI 1040 steel. They used the RSM method, for the prediction of Ra. In the same manner, Doniavi et al. [11] exploited the RSM approach to develop a mathematical model for predicting Ra. The authors proved that the f has a significant impact on the Ra variations. Kara et al. [12] presented a study based on ANN approach and the multiple regression analysis for modeling F_z during turning of AISI 316L stainless steel. The input parameters were V_c, f and coating type. The authors reported that the prediction results showed that ANN was the most efficient method compared to the multiple regression one, in terms of precision. Chabbi et al. [13] have compared two modeling methods RSM and ANN during the turning of polymer (POM C). They proved that models based on ANN are more precise than those dealing with RSM. Ranganathan et al. [14], performed a comparative modeling study between the methods RSM and ANN to predict Ra. during the turning of stainless steel (type 316) using tungsten carbide tool. Rafighi et al. [15] have presented the effects of cutting parameters (V_c, f, ap) and insert types on the surface roughness and cutting force components were investigated during hard turning of AISI D2 tool

steel. The RSM and ANN were used to determine the relationship between the input and output parameters. Fathallah et al. [16] have examined the benefits of the controlled grinding surface of the AISI D2 steel. The effect of Sol-gel abrasive wheel and cryogenic cooling mode on surface integrity have been examined. Gupta et al. [17] have been examined a comparative study between the methods ANN, SVR and RSM during turning. The results showed that the models ANN and SVR are much better than the models RSM in predicting surface roughness, tool wear and power. Fathallah et al. [18] conducted an experimental study to evaluate the average roughness of the peak-valley profile (Rz) and tangential cutting force Ft when machining cobalt alloys (Stellite 6). The ANN, SVM and RSM have been applied to model the results as a function of the operating parameters.

In this framework, the objective of the present research work is to compare the two modeling methods RSM and ANN when dealing with the cutting of AISI D3 tool steel with a triple coated carbide insert. The prediction models of cutting force and power consumption found by the two precited approachs are compared and discussed. Also, to highlight the relationship between cutting parameters tool radius (r), cutting speed (V_c), feed rate (f) and cutting depth (ap) and selected responses which are cutting speed and cutting power a design of experimental based on Taguchi L16 method was adopted.

2 Experimental Procedure

The experiments were carried out on a SN 40C lathe hat develops a spindle power of 6.6 kW. The turning operations were performed on AISI D3 cold-work tool steel specimens having a length of 350 mm, a diameter of 70 mm and a hardness $HB = 250$. Specimens were constituted of 2.00% C; 0.31% Si; 0.259% Ni; 0.124% Mo; 0.29% Mn; 0.009% S; 0.011% P; 0.162% Cu; and 12.00% Cr. The carbide inserts were CVD multi-layer coated carbide tool (Al_2O_3+TiC+TiCN) and secured on a PSBNR25×25M12 tool holder. Their active part geometry is: clearance angle (α) = 6°, rake angle (γ) = −6°, cutting edge inclination angle (λ) = −6°, the major cutting edge angle (χ) = 75°. A dynamometer (KISTLER 9257 B) was employed for the measurement of the tangential cutting force (F_z) (Fig. 1). It should be noted that the power consumed during machining is calculated using Eq. 1 based on the measured tangential force and the cutting speed.

$$P_c = \frac{F_z V_c}{60}\ , \text{[W]}. \tag{1}$$

A Taguchi experimental design L16 ($4 \wedge 3\ 2 \wedge 1$) was adopted for the reduction of the number of experiments. Four levels are designated for the three process factors

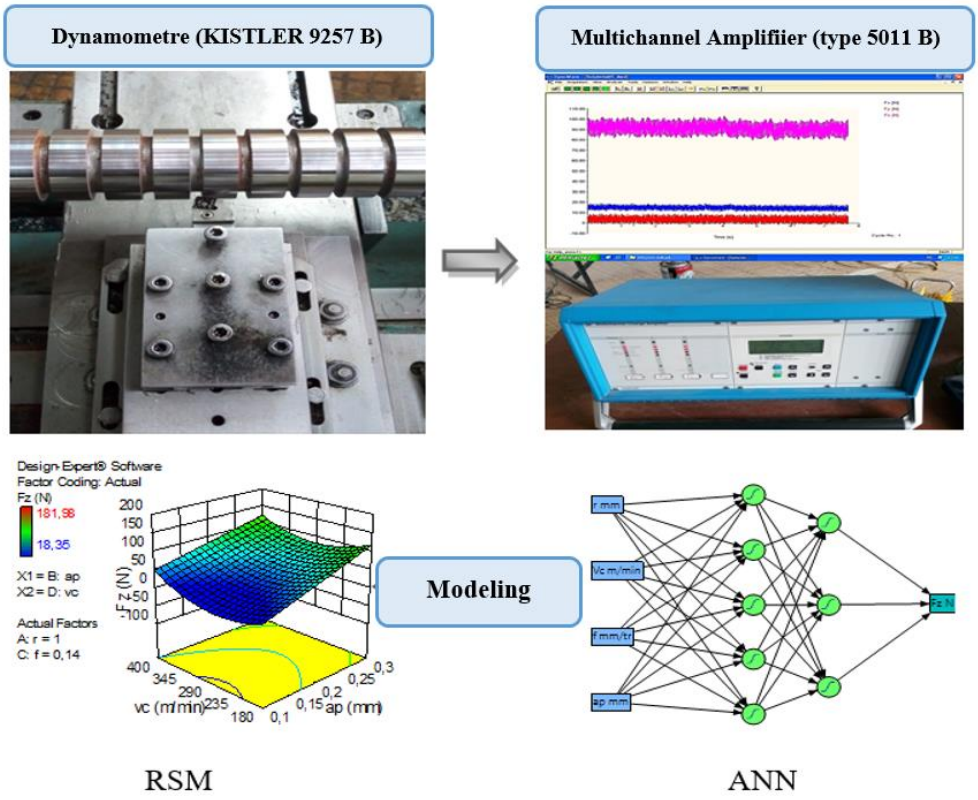

Fig. 1: Experimental setup and modeling methods adopted.

represented by r, f and V_c while only two levels for assigned to ap as presented in Table 1.

Table 1: Factor levels

		Levels			
		1	2	3	4
r	[mm]	0.4	0.8	1.2	1.6
V_c	[m/min]	180	255	330	400
f	[mm/rev]	0.08	0.12	0.16	0.20
ap	[mm]	0.1	0.3	—	—

3 Results and Discussion

Table 2 shows the resulting output parameters in terms of the variation of the input factors. It may be seen that the cutting force (F_z) varies from 18.35 N to 178.98 N, and that the power consumed (P_c) ranges from 55.05 W to 800.933 W.

Table 2: Experimental results

Trail	Cutting conditions				Response factors	
no.	r	V_c	f	ap	F_z	P_c
1	0.4	180	0.08	0.1	18.35	55.05
2	0.4	255	0.12	0.1	33.32	141.61
3	0.4	330	0.16	0.3	112.18	616.99
4	0.4	400	0.20	0.3	120.14	800.93
5	0.8	180	0.12	0.3	120.07	360.21
6	0.8	255	0.08	0.3	79.73	338.85
7	0.8	330	0.20	0.1	70.60	388.30
8	0.8	400	0.16	0.1	48.93	326.20
9	1.2	180	0.16	0.1	39.15	117.45
10	1.2	255	0.20	0.1	87.90	373.57
11	1.2	330	0.08	0.3	92.88	510.84
12	1.2	400	0.12	0.3	103.91	692.73
13	1.6	180	0.20	0.3	178.98	536.94
14	1.6	255	0.16	0.3	140.13	595.55
15	1.6	330	0.12	0.1	31.49	173.19
16	1.6	400	0.08	0.1	34.89	232.60

3.1 Response surface methodology (RSM)

The Response Surface Methodology (RSM) was used along with the Analysis Of Variance (ANOVA) procedure to carry out the statistical study and determine the contribution of the main parameters and their interactions [19].

The ANOVA Tables are expressed using:

— The degrees of freedom (DF).

— The sum of the squares (SS) of the variations from the mean is shown (Eq. 2):

$$SS_f = \frac{N}{N_{nf}} \sum_{i-1}^{N_{nf}} (\bar{y}_i - \bar{y})^2 \ . \tag{2}$$

— The contribution of the factors expressed as a percentage of the total variation and indicates the degree of impact on the result (Eq. 3):

$$\text{Cont}\% = \frac{SC_f}{SC_T} \times 100\,. \tag{3}$$

— The mean squares (MS) taken as the report of the SS to the DF (Eq. 4):

$$MS = \frac{SS_i}{DF_i}\,. \tag{4}$$

— The F-value obtained by the application of Eq. (5):

$$\text{F}_i = \frac{MC_i}{MS_e}\,. \tag{5}$$

— The P value shows the probability that represents the significance of the results obtained. If P is inferior to 0.05, the factor is considered significant. If P is superior to 0.05, the factor is then considered not significant.

3.1.1 Modeling of F_z and P_c using RSM

The ANOVA results for F_z illustrated in Table 3 show that ap and f are the most influential parameters for F_z variation with contributions of 67.55% and 22.15%, respectively. Similar results were reported by [20, 21]. They are followed by r and V_c with contributions reaching 3.79% and 1.30%. However, in the present case, the interactions did not show any significant influence. This is reason why they have been eliminated when elaborating Eq. (6).

Table 3: ANOVA for F_z

Source	DF	Seq SS	Cont. %	MS	F-Value	P-Value
r	1	1193.6	3.79%	1193.6	8.00	0.016
V_c	1	408.9	1.30%	408.9	2.74	0.126
f	1	6973.4	22.15%	6973.4	46.73	0.000
ap	1	21271.5	67.55%	21271.5	142.55	0.000
Error	11	1641.4	5.21%	149.2		
Total	15	31488.8	100.00%			

Table 4 illustrates the ANOVA results obtained for P_c. It can be observed that ap is the most influential factor on P_c with a contribution of 60.88%. It is followed by V_c and f with successive contributions of 17.67% and 17.55%. The radius r did not show any significant contribution, as found by [22].

Table 4: ANOVA for P_c

Source	DF	Seq SS	Cont. %	MS	F-Value	P-Value
r	1	34	0.00%	1978	1.07	0.325
V_c	1	126924	17.67%	126924	68.78	0.000
f	1	126060	17.55%	126568	68.59	0.000
ap	1	437275	60.88%	435017	235.75	0.000
$V_c \times ap$	1	9508	1.32%	9508	5.15	0.047
Error	10	18452	2.57%	1845		
Total	15	718254	100.00%			

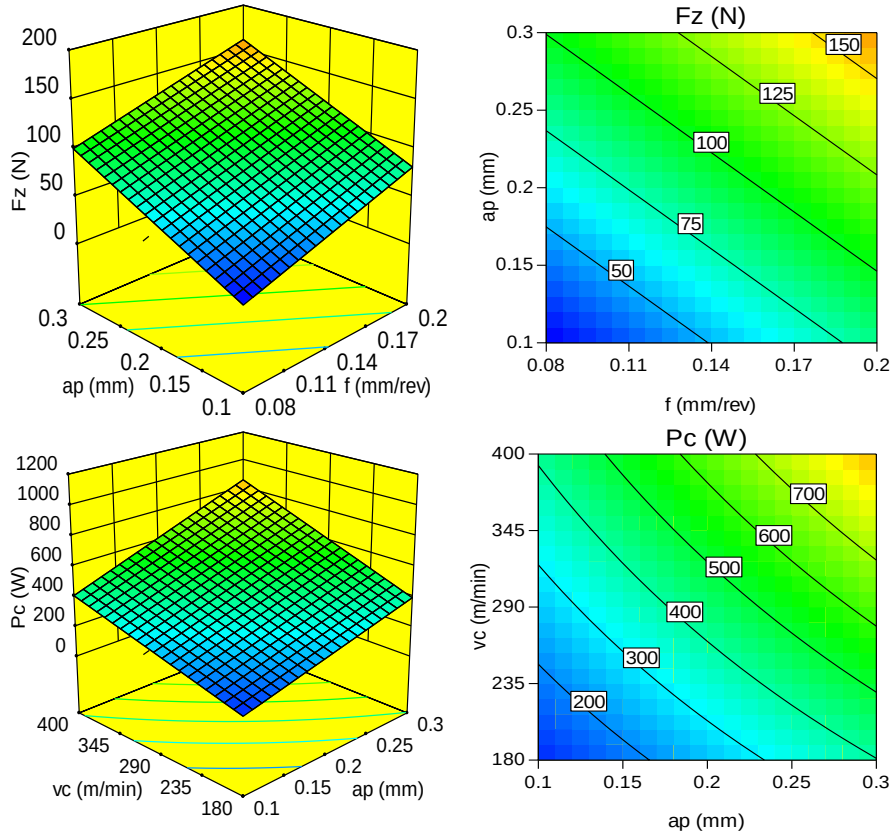

Fig. 2: 3D surface and contour graph of F_z and P_c using RSM.

The relation between the input and output factors was modeled by a regression equation that considers solely the terms of the main parameters (i.e. r, V_c, f and ap) and by taking into account the significant interactions in terms of the main parameters. Equations (6) and (7) illustrate the model developed leading to a determination coefficient R reaching 94.79 and 97.43% for F_z and P_c, respectively.

$$F_z = -57.6 + 19.31r - 0.0615V_c + 466.8f + 364.6ap\,, \tag{6}$$

$$P_c = -371.9 + 27.1r + 0.436V_c + 1989f + 710ap + 3.24V_cap\,. \tag{7}$$

Figure 2 illustrates the three-dimensional response surface showing contour of F_z in terms of the two experimental factors (ap and f). It can be seen that any augmentation of these two factors leads to a similar augmentation in F_z. This rise can indeed be justified by the growth in the chip section removed that requires a high amount of cutting effort.

The 3D surfaces and contours are representing P_c based of the input factors (ap and V_c) as shown in figure (2). It can be observed that the increase in the (ap) and V_c generates an increase in P_c. These results are found to correlate those reported in [23].

3.2 Artificial neural networks (ANN)

The ANN approach have been developed to solve problems in different domains for regression modeling. This technique provides the mathematical formulation of non-linear problems. The most frequently applied neurons are those for that the transfer function f is a non-linear function (generally a hyperbolic tangent) of a linear combination of the inputs (Eq.8) [24]

$$f = \tanh \sum_{i=1}^{n} w_i x_i \tag{8}$$

with x_i are the input variables of the neuron, the w_i are adjustable parameters and n is the number of neurons.

3.2.1 Modeling of F_z and P_c using ANN method

Figure 3 shows an input layer of 4 nodes representing the input parameters, two hidden layers and an output layer (4-5-3-1). The training run rate adopted for processing all output technology parameters is $\eta = 0.1$ with a maximum number of iterations of 100. In order to model F_z, 16 tests were performed and separated into two groups. The first group comprised 12 tests for neural network training while the second applied 4 tests for validation. For P_c modeling, 13 out of 16 trials were adopted for

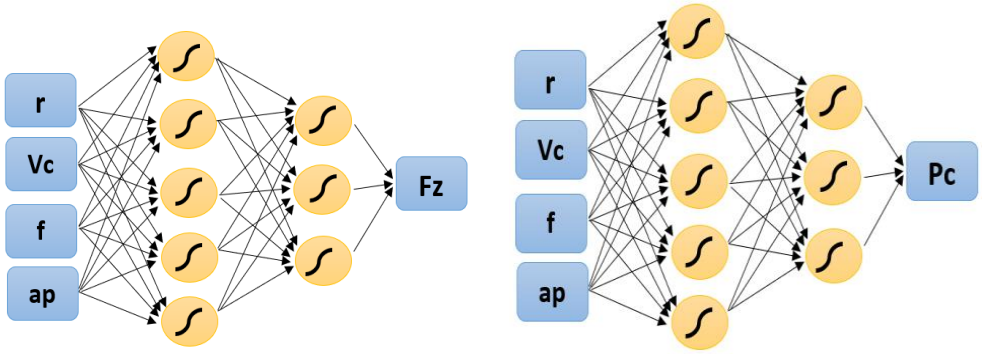

Fig. 3: ANN structure (4-5-3-1) for F_z and P_c.

training the ANN while 3 trials were randomly selected to check the effectiveness of the network. Several network structures were tested and only the structure that gave the best result was chosen.

The application of the ANN method resulted in an equation (Eq. 9) representing the mathematical model of F_z. For the output layer

$$F_z = 3.802\text{HH1} - 21.739\text{HH2} + 110.525\text{HH3} + 93.338\,. \tag{9}$$

For the hidden layer

$$\begin{aligned}
\text{HH1} &= \tanh(0.5(-0.234\text{H1} - 0.296\text{H2} + 0.117\text{H3} - 0.302\text{H4} - 0.023\text{H5} + 0.178));\\
\text{HH2} &= \tanh(0.5(0.546\text{H1} - 0.336\text{H2} + 0.266\text{H3} + 0.165\text{H4} - 0.025\text{H5} - 0.511));\\
\text{HH3} &= \tanh(0.5(-0.958\text{H1} - 0.860\text{H2} - 0.614\text{H3} + 0.057\text{H4} - 1.819\text{H5} + 0.647));\\
\text{H1} &= \tanh(0.5(1.480r - 0.007V_c - 17.955f - 7.740ap + 4.141));\\
\text{H2} &= \tanh(0.5(0.883r - 0.009V_c + 24.436f - 3.333ap - 0.733));\\
\text{H3} &= \tanh(0.5(-2.532r - 0.007V_c - 11.775f - 4.331ap + 7.229));\\
\text{H4} &= \tanh(0.5(0.338r - 0.005V_c - 3.718f + 1.144ap + 1.285));\\
\text{H5} &= \tanh(0.5(0.097r + 0.012V_c - 17.918f - 6.253ap + 1.700)).
\end{aligned}$$

Equation (10) illustrates the mathematical model developed for P_c

$$P_c = -569.4255HH1 + 649.878HH2 - 1202.898HH3 + 1152.178\,. \tag{10}$$

For the hidden layer

$$\text{HH1} = \tanh(0.5(0.685\text{H1} + 0.780\text{H2} + 0.703\text{H3} - 0.612\text{H4} - 1.044\text{H5} + 1.601));$$

$$\text{HH2} = \tanh(0.5(0.952\text{H1} - 0.499\text{H2} - 0.055\text{H3} - 1.084\text{H4} - 0.592\text{H5} + 1.754));$$
$$\text{HH3} = \tanh(0.5(2.151\text{H1} - 0.607\text{H2} - 0.074\text{H3} + 0.442\text{H4} - 1.152\text{H5} + 1.252));$$
$$\text{H1} = \tanh(0.5(1.002r - 0.009V_c - 8.096f - 0.819ap + 2.259));$$
$$\text{H2} = \tanh(0.5 \times 4.455r - 0.014V_c + 9.884f + 22.207ap - 7.131));$$
$$\text{H3} = \tanh(0.5(-0.466r - 0.017V_c + 3.981f - 2.586ap + 5.995));$$
$$\text{H4} = \tanh(0.5(-2.594r + 0.013V_c - 22.575f - 26.094ap + 6.883));$$
$$\text{H5} = \tanh(0.5(1.062r - 0.001V_c + 15.814f + 1.557ap - 6.520)).$$

From the ANN model (Eqs. 9 and 10), Figure 4 illustrates the 3D response surface with the contour of F_z and P_c in terms of the two experimental factors (ap and f). It may be noted that any augmentation in these two factors results to a similar rise in F_z and P_c. As a result, the minimum cutting force and power consumption are obtained for a minimum value of ap and f.

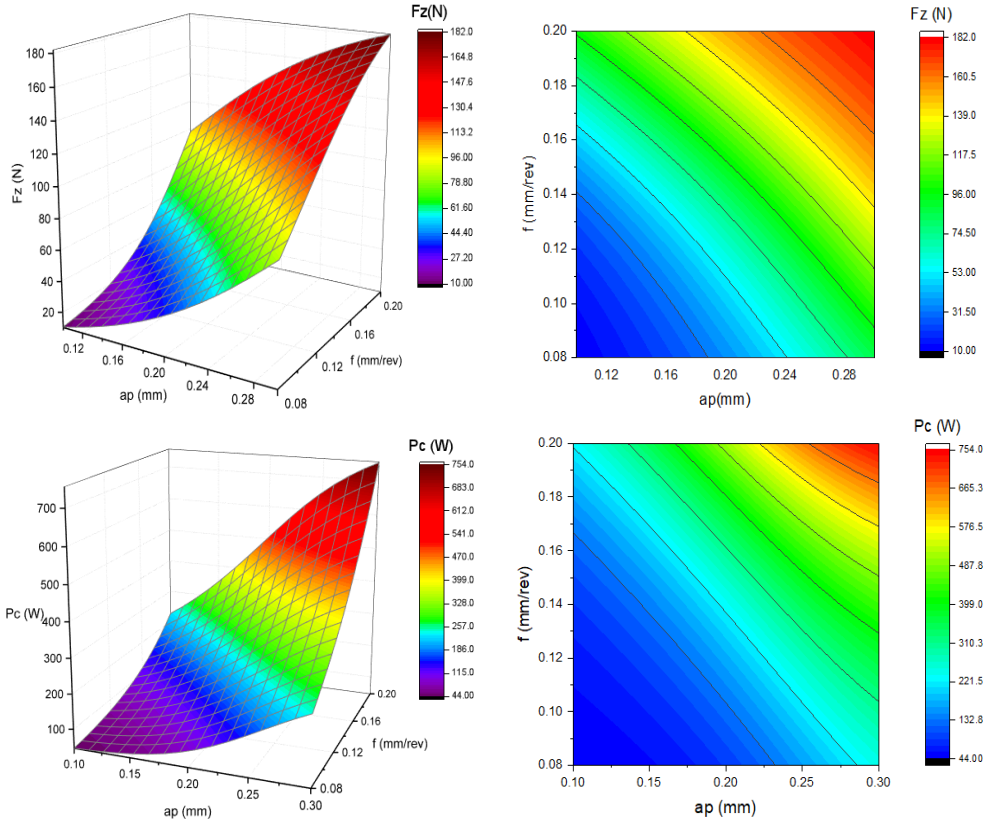

Fig. 4: 3D surface and contour graph of F_z and P_c using ANN method.

Tables 5 and 6 illustrate the determination coefficient (R), the root mean square error (RMSE) and the number of tests performed for the training and validation cases of F_z and P_c.

Table 5: R, RMSE and tests number of F_z model

F_z	Training	Validation
R	99.99	99.99
RMSE	0.118322	0.0394637
Number of tests	12	4

Table 6: R, RMSE and tests number of P_c model

P_c	Training	Validation
R	99.96	100
RMSE	5.02	0.0009
Number of tests	13	3

Figure 5 illustrates the ANN experimental results against the predicted values for the training and validation cases. Both F_z and P_c show a linear variation that

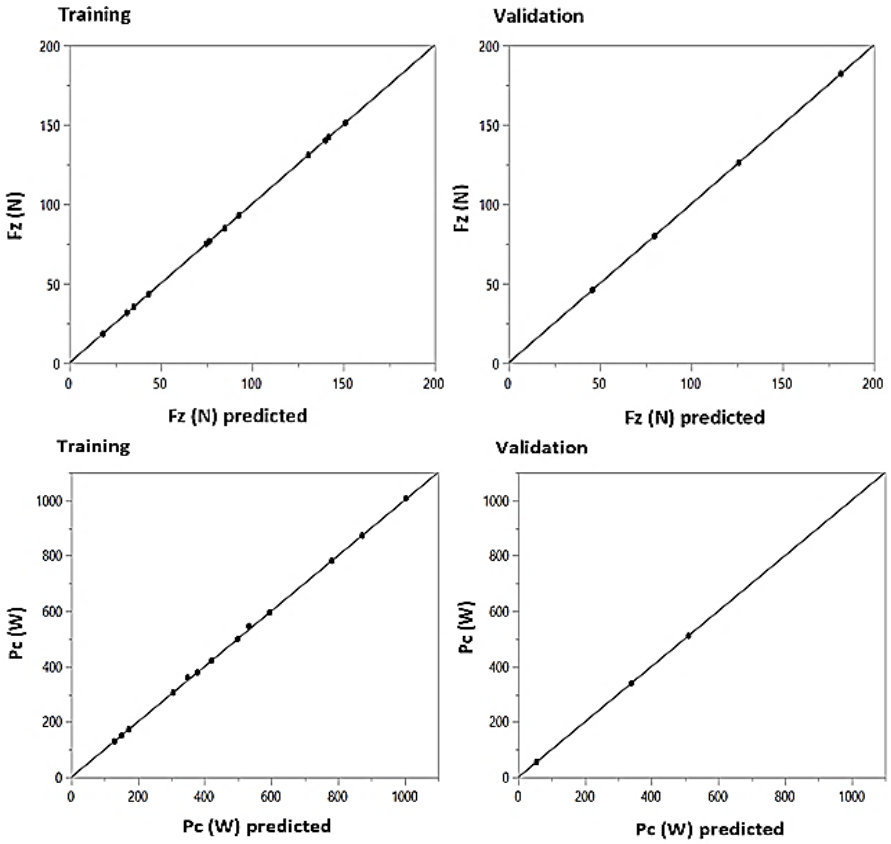

Fig. 5: Comparison between experimental and predicted values for F_z and P_c.

indicates that the mathematical models developed for F_z and P_c are adequate. This is a demonstration of the accuracy of the two mathematical model.

3.3 Comparison between RSM and ANN models

The comparison between the RSM and the ANN models when applied to the F_z and P_c are presented in Table 7 in terms of the determination coefficient R and the RMSE.

The results predicted by both RSM and ANN models are compared to the experimental results in Fig. 6.

The analysis of the results clearly shows that the mathematical models obtained

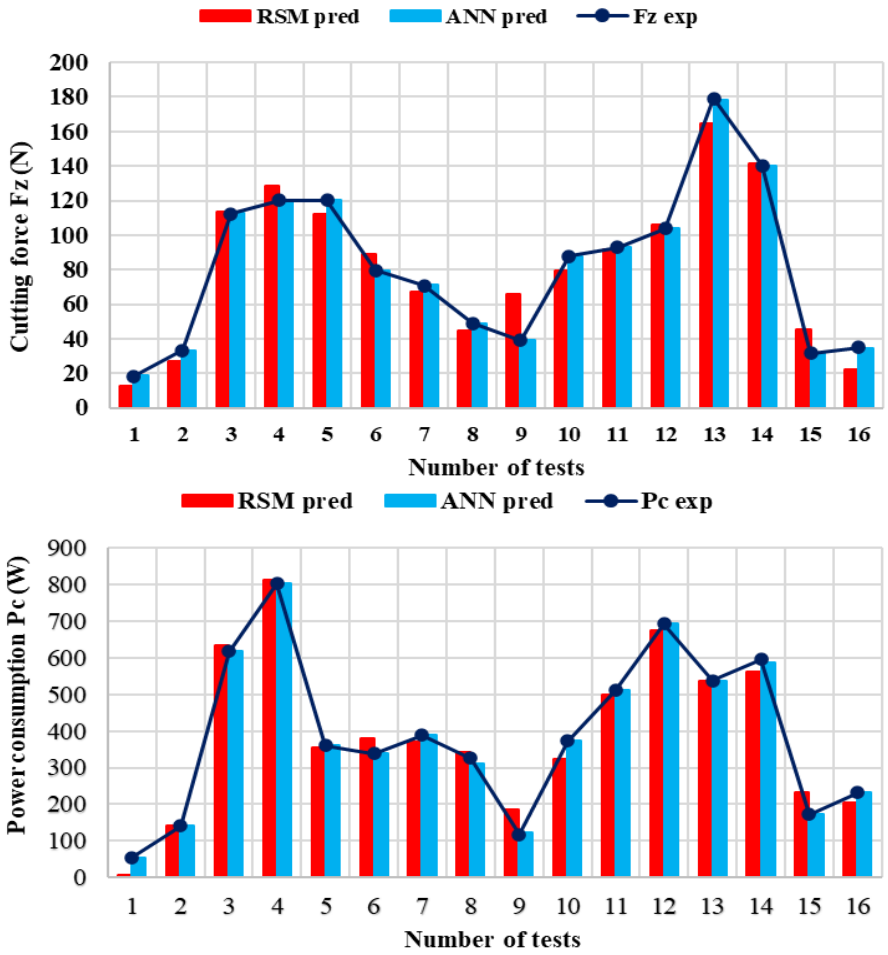

Fig. 6: Experimental, RSM and ANN predicted results for F_z and P_c.

by both methods are satisfactory. It can be underlined that ANN models being usually more accurate than the RSM as reported by [25, 26]. Concerning F_z, Table 7 shows that (R $=$ 99.99% and RMSE $=$ 0.098%) for ANN models. They are considered preferable to those presented by the RSM models (R $=$ 94.79% and RMSE $=$ 7.912%). Similar results are reported for P_c where the ANN models again

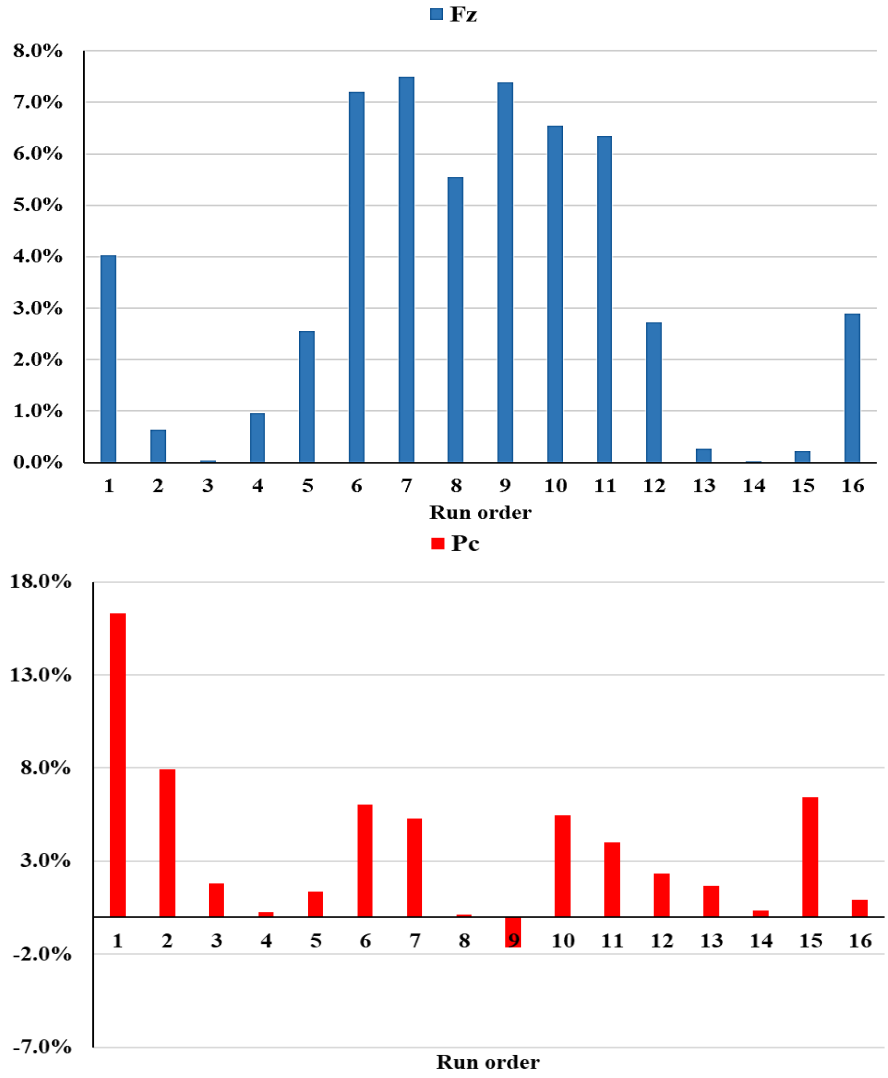

Fig. 7: Benefit in terms of precision percent offered by ANN model compared with RSM model for P_c and F_z.

Table 7: Comparison between RSM and ANN models

	RI		RMSE	
Responses	RSM	ANN	RSM	ANN
F_z	94.79	99.99	7.912	0.098
P_c	97.43	99.97	27.127	4.078

better results (R $= 99.97\%$ and RMSE $= 4.078\%$) compared to RSM (R $= 97.43\%$, RMSE $= 27.127\%$). Consequently, both proposed models may be used effectively for predicting both F_z and P_c during turning process of AISI D3 steel machined with triple coated carbide tool.

The ANN prediction model provides the maximum benefit in terms of precision compared to the RSM model. For the effort F_z the benefit is equal to 7.5% and for P_c it is equal to 16.3%, as shown in Fig. 7.

4 Validation Tests

The validation step is necessary to verifying the adequacy of the mathematical models. This was done by performing an additional test with different cutting conditions than those represented in Table 8. The validation results achieved lead to confirm the consistency of the models derived by both ANN and RSM, and also to certify the reliability of ANN models over those of RSM in terms of prediction.

Table 8: Confirmation test results

	Cutting conditions				Experimental results		Predicted results		Error [%]	
	r	V_c	f	ap	F_z	P_c	F_z	P_c	F_z	P_c
RSM	0.8	330	0.08	0.3	98.64	542.52	84.28	486.54	14.5	10.3
ANN	0.8	330	0.08	0.3	98.64	542.52	97.32	547.64	1.3	0.9

5 Conclusions

Experimental and modeling studies of cutting force and power consumption variations were carried out in this reseach work based on two statistical methods RSM and ANN. The case of the machining of AISI D3 cold work tool steel with a CVD triple coated carbide cutting tool Al_2O_3+TiC+TiCN is treated. Based on obtained results, the following conclusions can be highlighted:

The ANOVA procedure demonstrated that any augmentation in ap and f led to an augmentation of F_z with contributions of 67.55 and 22.15%, respectively.

The ANOVA for P_c demonstrated that any augmentation in ap, V_c and f led to an augmentation of P_c with contributions 60.88, 17.67, and 17.55%, respectively.

The comparison between the RSM and the ANN models in terms of the parameters considered represented by R and RMSE shows that, for a limited number of experiments, the ANN models were able to predict the response with greater accuracy, i.e.

$$\begin{aligned} \mathrm{R_{ANN}}(F_z) = 99.99\% \text{ and } \mathrm{R_{ANN}}(P_c) = 99.97\%; \\ \mathrm{R_{RSM}}(F_z) = 94.79\% \text{ and } \mathrm{R_{RMS}}(P_c) = 97.43\%; \\ \mathrm{RMSE_{ANN}}(F_z) = 0.098\% \text{ and } \mathrm{RMSE_{ANN}}(P_c) = 4.078\%; \\ \mathrm{RMSE_{RSM}}(F_z) = 7.912\% \text{ and } \mathrm{RMSE_{RMS}}(P_c) = 27.127\%. \end{aligned}$$

The ANN prediction model provides a maximal benefit in terms of precision of F_z which is egual to 7.5% and of P_c which is also egual to 16.3% compared with the RSM prediction model.

The mathematical models developed were found to agree with the experimental data. These models should be of great interest to mechanical manufacturers as they are capable of providing accurate predictions thus leading to substantial gains in time and material.

ACKNOWLEDGEMENT

The present research was undertaken by the "Metal Cutting Research Group" of the Structures and Mechanics Laboratory (LMS) of the 8 May 1945-Guelma University, Algeria, and received funding from the General Directorate of Scientific Research and Technological Development (DGRSDT) under the PRFU research project A11N01UN240120190001.

REFERENCES

[1] M.A. YALLESE, J.F. RIGAL, K.CHAOUI, L. BOULANOUAR (2005) The effects of cutting conditions on mixed ceramic and cubic boron nitride tool wear and on surface roughness during machining of X200Cr12 steel (60 HRC). *Proceedings of the Institution of Mechanical Engineers, Part B: Journal of Engineering Manufacture* **219**(1) 35-55.

[2] H. BOUCHELAGHEM, M.A. YALLESE, A. AMIRAT, S. BELHADI (2007) Wear behavior of CBN tool when turning hardened AISI D3 steel. *Mechanics* **65**(3) 57-65.

[3] A.M. ZAIN, H. HARON, S. SHARIF (2010) Prediction of surface roughness in the end milling machining using Artificial Neural Network. *Expert Systems with Applications* **37**(2) 1755-1768.

[4] I. MEDDOUR, M.A. YALLESE, H. BENSOUILAH, A. KHELLAF, M. ELBAH (2018) Prediction of surface roughness and cutting forces using RSM, ANN, and NSGA-II in

finish turning of AISI 4140 hardened steel with mixed ceramic tool. *The International Journal of Advanced Manufacturing Technology* **97**(5) 1931-1949.

[5] R. SURESH, A.G. JOSHI, M. MANJAIAH (2021) Experimental Investigation on tool wear in AISI H13 die steel turning using RSM and ANN methods. *Arabian Journal for Science and Engineering* **46**(3), 2311-2325.

[6] R. KUMAR, A.K. SAHOO, P.C. MISHRA, R.K. DAS, S. ROY (2018) ANN Modeling of Cutting Performances in Spray Cooling Assisted Hard Turning. *Materials Today: Proceedings* **5**(9) 18482-18488.

[7] R.F. MEKNASSI (2019) Etude de l'impact des conditions de coupe lors du tournage des polyamides avec renfort en fibre de verre (PA66/GF30) en utilisant les méthodes RSM et ANN.

[8] U.M.R. PATURI, H. DEVARASETTI, S.K.R. NARALA (2018) Application of regression and artificial neural network analysis in modelling of surface roughness in hard turning of AISI 52100 steel. *Materials Today: Proceedings* **5**(2) 4766-4777.

[9] V.N. GAITONDE, S.R. KARNIK, L. FIGUEIRA, J.P. DAVIM (2009) Analysis of machinability during hard turning of cold work tool steel (type: AISI D2). *Materials and Manufacturing Processes* **24**(12) 1373-1382.

[10] S. NEŞELI, S. YALDIZ, E. TÜRKEŞ (2011) Optimization of tool geometry parameters for turning operations based on the response surface methodology. *Measurement* **44**(3) 580-587.

[11] A. DONIAVI, M. ESKANDERZADE, M. TAHMSEBIAN (2007) Empirical modeling of surface roughness in turning process of 1060 steel using factorial design methodology. *Journal of Applied Sciences* **7**(17) 2509-2513.

[12] F. KARA, K. ASLANTAS, A. IEK (2015) ANN and multiple regression method-based modelling of cutting forces in orthogonal machining of AISI 316L stainless steel. *Neural Computing and Applications* **26**(1) 237-250.

[13] A. CHABBI, M.A. YALLESE, M. NOUIOUA, I. MEDDOUR, T. MABROUKI, F. GIRARDIN (2017) Modeling and optimization of turning process parameters during the cutting of polymer (POM C) based on RSM, ANN, and DF methods. *The International Journal of Advanced Manufacturing Technology* **91**(5) 2267-2290.

[14] S. RANGANATHAN, ET AL. (2010) 'Evaluation of machining parameters of hot turning of stainless steel (Type 316) by applying ANN and RSM'. *Materials and manufacturing processes* **25** 1131-1141.

[15] M. RAFIGHI, M. ÖZDEMIR, S. AL SHEHABI, M.T. KAYA (2021) Sustainable hard turning of high chromium AISI D2 tool steel using CBN and ceramic inserts. *Transactions of the Indian Institute of Metals* **74**(7) 1639-1653.

[16] B.B. FATHALLAH, C. BRAHAM, H. SIDHOM (2020) Combined effects of abrasive type and cooling mode on fatigue resistance of AISI D2 ground surface. *International Journal of Fatigue* **138** 105665.

[17] A.K. GUPTA (2010) Predictive modelling of turning operations using response surface methodology, artificial neural networks and support vector regression. *International Journal of Production Research* **48**(3) 763-778.

[18] B.B. FATHALLAH, R. SAIDI, S. BELHADI, M.A. YALLESE, T. MABROUKI (2021) Modelling of cutting forces and surface roughness evolutions during straight turning of Stellite 6 material based on response surface methodology, artificial neural networks and support vector machine approaches. *Journal of Mechanical Engineering and Sciences* **15**(4) 8540-8554.

[19] I. ASILTRK, M. ÇUNKAŞ (2011) Modeling and prediction of surface roughness in turning operations using artificial neural network and multiple regression method. *Expert systems with applications* **38**(5) 5826-5832.

[20] R. SURESH, S. BASAVARAJAPPA, G.L. SAMUEL (2012) Some studies on hard turning of AISI 4340 steel using multilayer coated carbide tool. *Measurement* **45**(7) 1872-1884.

[21] O. ZERTI, M.A. YALLESE, R. KHETTABI, K. CHAOUI, T. MABROUKI (2017) Design optimization for minimum technological parameters when dry turning of AISI D3 steel using Taguchi method. *International Journal of Advanced Manufacturing Technology* **89**(5) 1915-1934.

[22] S. CHINCHANIKAR, S.K. CHOUDHURY (2013) Effect of work material hardness and cutting parameters on performance of coated carbide tool when turning hardened steel: An optimization approach. *Measurement* **46**(4) 1572-1584.

[23] R.K. BHUSHAN (2013) Optimization of cutting parameters for minimizing power consumption and maximizing tool life during machining of Al alloy SiC particle composites. *Journal of Cleaner Production* **39** 242-254.

[24] M. GOPAL (2021) The Effect of Machining Parameters and Optimization of Temperature Rise in Turning Operation of Aluminium-6061 Using RSM and Artificial Neural Network. *Periodica Polytechnica Mechanical Engineering* **65**(2) 141-150.

[25] H. TEBASSI, M.A. YALLESE, I. MEDDOUR ET AL (2017) On the modeling of surface roughness and cutting force when turning of Inconel 718 using artificial neural network and response surface methodology: accuracy and benefit. *Periodica Polytechnica Mechanical Engineering* **61**(1) 1-11.

[26] A. LABIDI, H. TEBASSI, S. BELHADI, R. KHETTABI, M.A. YALLESE (2018) Cutting conditions modeling and optimization in hard turning using RSM, ANN and desirability function. *Journal of Failure Analysis and Prevention* **18**(4) 1017-1033.